Journal of Power Sources 189 (2009) 629–632

Contents lists available at ScienceDirect

Journal of Power Sources

journal homepage: www.elsevier.com/locate/jpowsour

Short communication

All-solid-state lithium secondary batteries using nanocomposites of NiS electrode/Li_2S–P_2S_5 electrolyte prepared via mechanochemical reaction

Yusuke Nishio, Hirokazu Kitaura, Akitoshi Hayashi*, Masahiro Tatsumisago

Department of Applied Chemistry, Graduate School of Engineering, Osaka Prefecture University, 1-1 Gakuen-cho, Naka-ku, Sakai, Osaka 599-8531, Japan

ARTICLE INFO

Article history:
Received 30 July 2008
Received in revised form
11 September 2008
Accepted 15 September 2008
Available online 27 September 2008

Keywords:
All-solid-state battery
Lithium battery
Solid electrolyte
Nanocomposite
Electrode–electrolyte interface

ABSTRACT

All-solid-state batteries have been desired for the purpose of safety improvement of lithium secondary batteries. In order to improve performance of all-solid-state cells, the formation technique of a favorable interface between active materials and solid electrolytes should be developed. The nanocomposite of the NiS active material and the $80Li_2S{\cdot}20P_2S_5$ (mol%) electrolyte was synthesized via a mechanochemical reaction and applied as an electrode to all-solid-state lithium secondary cells. The capacity of the cell with the nanocomposite electrode was larger than that with an electrode prepared by hand-mixing of the active material and the electrolyte powder at both current densities of 64 $\mu A\,cm^{-2}$ and 1.28 $mA\,cm^{-2}$. The cell with the nanocomposite showed 360 $mAh\,g^{-1}$ after 50 cycles at 1.28 $mA\,cm^{-2}$ in the potential range from 1.0 to 4.0 V vs. Li.

© 2008 Elsevier B.V. All rights reserved.

1. Introduction

Lithium-ion batteries have been used as power sources for a wide range of portable devices because of high operating voltage, high energy density, light weight and longer cycle life. Recently, lithium-ion batteries with large-scale for electric vehicles have attracted much attention and thus the improvements in safety of lithium-ion batteries are demanded. It is expected that all-solid-state lithium secondary batteries without a flammable liquid electrolyte have a high safety and reliability. Solid electrolytes are the key-materials for all-solid-state batteries. The Li_2S–P_2S_5 glass and glass-ceramic as a solid electrolyte exhibits high Li^+ ion conductivity of 10^{-4} to 10^{-3} $S\,cm^{-1}$ at room temperature [1]. In the all-solid-state cells, the composite electrodes consisted of active materials, solid electrolytes (Li^+ ion conduction path) and conductive additives (electron conduction path) are used [2,3]. The performance of the all-solid-state cells is influenced significantly by the mixture state of composite electrodes. It is also difficult for all-solid-state cells to operate at high current densities because the solid-solid contact between active materials and electrolytes is not sufficient. In order to improve performance of all-solid-state cells, the formation technique of a favorable interface between active materials and solid electrolytes should be developed.

Among various candidates for positive electrode materials, sulfur and metal sulfides are known to be promising because of their low cost and high theoretical capacity [4–6]. However, the cells using sulfur or metal sulfide as an electrode material cause a rapid capacity fading during cycling because soluble lithium polysulfides, which are formed during a discharge process, are dissolved in liquid electrolytes. Nickel sulfide (NiS) has a good electronic conductivity and a high theoretical capacity of 590 $mAh\,g^{-1}$ [7–9]. It is expected that the cyclability of the cells with nickel sulfide is improved by using inorganic solid electrolytes because the dissolution of polysulfides is suppressed.

We have reported that the NiS–$80Li_2S{\cdot}20P_2S_5$ nanocomposites, in which NiS nanoparticles as an active material were embedded in the $80Li_2S{\cdot}20P_2S_5$ (mol%) glass matrix as a solid electrolyte, were synthesized by mechanical milling [10]. All-solid-state cells using the composite as a positive electrode worked as rechargeable batteries. In this study, morphology and electrochemical properties of the nanocomposite electrode were compared with those of a hand-mixed-electrode which was prepared by hand-mixing of the active material and the electrolyte powder. Effects of the addition of acetylene black as a conductive additive to the nanocomposite electrode on the cell performance were investigated in all-solid-state cells. Reaction mechanism of the NiS active material in the cells was examined by *ex situ* XRD measurements.

* Corresponding author. Tel.: +81 72 254 9334; fax: +81 72 254 9334.
E-mail address: hayashi@chem.osakafu-u.ac.jp (A. Hayashi).

0378-7753/$ – see front matter © 2008 Elsevier B.V. All rights reserved.
doi:10.1016/j.jpowsour.2008.09.064

2. Experimental

The Ni_3S_2 and NiS powders were synthesized by ball milling from elemental sulfur (Kojundo Chem. Lab Co., 99.99%) and nickel metal (Kojundo Chem. Lab Co., 99.9%) powders under an Ar atmosphere. Pure nickel and sulfur powders were mixed with the molar ratio of 3:2 or 1:1, respectively and sealed in a hardened stainless steel vial in a glove box with Ar gas. Milling was conducted in a planetary ball mill (Pulerisette 7, Fritsch). Ten zirconia balls of 10 mm in diameter were used as a grinding media. The Ni_3S_2 and NiS crystals were prepared by milling for 24 h. The electrode–electrolyte nanocomposite was synthesized from trinickel disulfide Ni_3S_2 and lithium nitride Li_3N (Aldrich) as starting materials. A mixture of these two powders was milled for 2 h at a rotation speed 370 rpm to form the Ni–Li_2S nanocomposite powder, in which the Ni nanoparticles were dispersed in Li_2S matrix. Then sulfur S was added to the Ni–Li_2S nanocomposite and then the mixture was milled for 5 h at 370 rpm to form the NiS–Li_2S nanocomposite. Finally, P_2S_5 (Aldrich, 99%) was added to the NiS–Li_2S nanocomposite with the composition corresponding to the molar ratio of Li_2S:P_2S_5 = 80:20 and milled for 2 h at 370 rpm to form the NiS–$80Li_2S{\cdot}20P_2S_5$ (mol%) as electrode–electrolyte nanocomposite. The weight ratio of the NiS electrode and the $80Li_2S{\cdot}20P_2S_5$ glass electrolyte in the nanocomposite was 57:43. The NiS–$80Li_2S{\cdot}20P_2S_5$ nanocomposites added with acetylene black (AB) were also synthesized by the addition of AB and P_2S_5 at the same time. The amounts of additional AB were 4, 6 and 8 wt.% of the NiS–$80Li_2S{\cdot}20P_2S_5$ nanocomposite. The hand-mixed-electrodes were also prepared by mixing gently NiS prepared above and the $80Li_2S{\cdot}20P_2S_5$ glass [1], and in some cases acetylene black powders in the same proportion of the electrode–electrolyte nanocomposites described above.

The electrochemical properties of the NiS electrode–$80Li_2S{\cdot}20P_2S_5$ electrolyte nanocomposites were investigated in the all-solid-state cells. The two electrode cells were assembled using the nanocomposites or the hand-mixed-electrodes as a working electrode, the Li–In alloys as a counter electrode and the $80Li_2S{\cdot}20P_2S_5$ glass-ceramic [1] as a solid electrolyte in a dry Ar filled glove box. The working electrode powders (10 mg) and the solid electrolyte powder (80 mg) were placed in a polycarbonate tube (ϕ = 10 mm) and pressed under 360 MPa. The counter electrode, which was formed by attaching a lithium foil and an indium foil, was put on the surface of the solid electrolyte side of the bilayer pellet. Then the three-layered pellet was sandwiched by two stainless-steel rods as current collectors. The molar ratio of the Li/In is 0.79 in the counter electrode. When the molar ratio is less than 1, the potential of the Li–In alloys was reported to be constant at approximately 0.6 V vs. Li [2]. The potential difference of 0.6 V between Li–In and Li is used in this report. The cells were discharged and charged galvanostatically at 64 $\mu A\,cm^{-2}$ or 1.28 $mA\,cm^{-2}$ at 25 °C in an Ar atmosphere using a charge–discharge measuring device (BTS-2004, Nagano Co.). The working electrode in the cells discharged and charged was analyzed by *ex situ* X-ray diffraction measurements (Cu Kα) in an Ar atmosphere.

3. Results and discussions

The electrode–electrolyte nanocomposites were prepared by ball milling. XRD measurements showed the formation of NiS crystal in the nanocomposites (as shown in Fig. 5(a)). It was confirmed by ^{31}P MAS-NMR measurements that local structure around phosphorus atoms in the nanocomposite was similar to that in $80Li_2S{\cdot}20P_2S_5$ glass [10]. Fig. 1 shows the high angle annular dark field-scanning transmission electron microscope (HAADF-STEM) images of the NiS–$80Li_2S{\cdot}20P_2S_5$ nanocomposite electrode (a) and the hand-mixed-electrode of the NiS crystal and the $80Li_2S{\cdot}20P_2S_5$ glass (b). The bright and dark areas respectively denote the presence of NiS and Li_2S–P_2S_5 domains, which were supported by elemental analysis data. It is revealed that NiS particles are much more dispersed in the nanocomposite than in the mixture. The NiS particle size in the nanocomposite electrode is 10–500 nm, whereas the size of aggregated NiS particles in the hand-mixed-electrode is 0.1–2.0 μm. The contact area between NiS particles and the $80Li_2S{\cdot}20P_2S_5$ glass matrix of the nanocomposite is much larger than the mixture. Mechanochemical process is effective in forming a favorable interface between electrode and electrolyte.

Fig. 2 shows the initial charge–discharge curves of the cells using the NiS–$80Li_2S{\cdot}20P_2S_5$ nanocomposite and the mixture of the NiS crystal and the $80Li_2S{\cdot}20P_2S_5$ glass as a working electrode at 64 $\mu A\,cm^{-2}$. The cell with the nanocomposite electrode exhibits a much larger capacity than that with the hand-mixed-electrode. The discharge curves of both the nanocomposite and the hand-mixed-electrodes show a first plateau at 1.6–1.8 V vs. Li and a second plateau at 1.2–1.4 V vs. Li. These plateaus correspond to the plateaus observed in the cells using liquid and polymer electrolytes [7–9]. The discharge reaction mechanism in a Li/NiS cell is reported as follows:

$$NiS + (2/3)Li^+ + (2/3)e^- \rightarrow (1/3)Ni_3S_2 + (1/3)Li_2S \quad \text{(first plateau)}$$

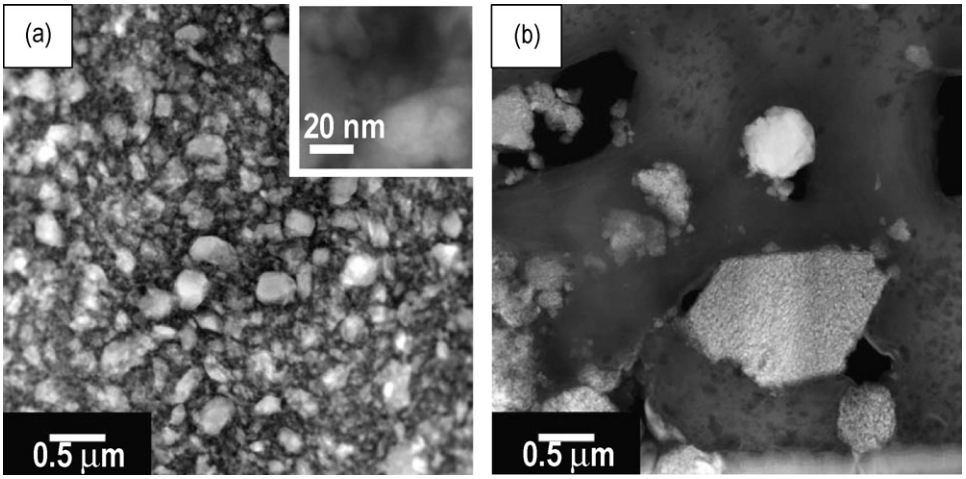

Fig. 1. The HAADF-STEM images of the NiS–$80Li_2S{\cdot}20P_2S_5$ nanocomposite (a) and the mixture (b). The inset in (a) is the magnified image of the nanocomposite.

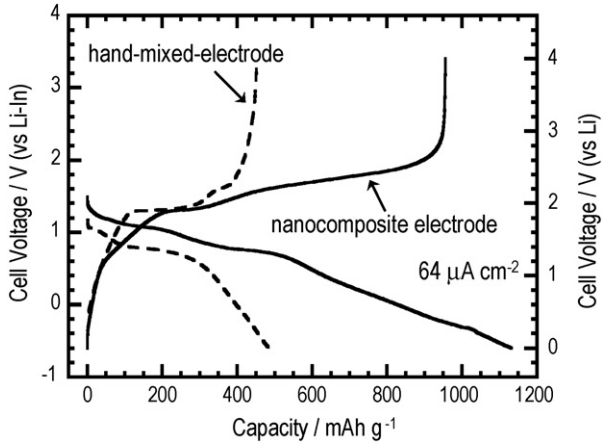

Fig. 2. The charge–discharge curves at 64 μA cm^{-2} of the cells with the nanocomposite electrode and the hand-mixed-electrode.

$$(1/3)Ni_3S_2+(4/3)Li^+ +(4/3)e^- \rightarrow Ni + (2/3)Li_2S \quad \text{(second plateau)}$$

The total discharge reaction is represented as follows:

$$NiS + 2Li^+ + 2e^- \rightarrow Ni + Li_2S$$

Although the nanocomposite shows a larger total capacity than the theoretical capacity of NiS (590 mAh g^{-1}), the capacity in the range of the two plateaus is almost the same as the theoretical capacity. The utilization ratio of the active material NiS in the nanocomposite is improved in comparison with the mixture. The sloping voltage down to 0 V, which is the cause of the large total capacity, would not be attributed to NiS electrode reaction; the capacity of sloping voltage has somewhat reversibility. The reaction mechanism for the sloping voltage region has not been clarified at the present stage.

Fig. 3 shows the charge–discharge curves at a higher current density of 1.28 mA cm^{-2} at the first cycle of the cells using the nanocomposite electrode of NiS–80Li_2S·20P_2S_5 without AB (a) and the NiS–80Li_2S·20P_2S_5-AB (b, c, d) which have 4, 6 and 8 wt.% AB, respectively. The cell performance of the hand-mixed-electrode of NiS, 80Li_2S·20P_2S_5 and 6 wt.% AB is also shown in Fig. 3(e). The discharge voltages of the cells at 1.28 mA cm^{-2} are lower than that of the cells at 64 μA cm^{-2} as shown in Fig. 1 and obvious plateaus are not observed. The charge–discharge curves of the cells using the nanocomposites with 0 and 4 wt.% AB are almost the same and the

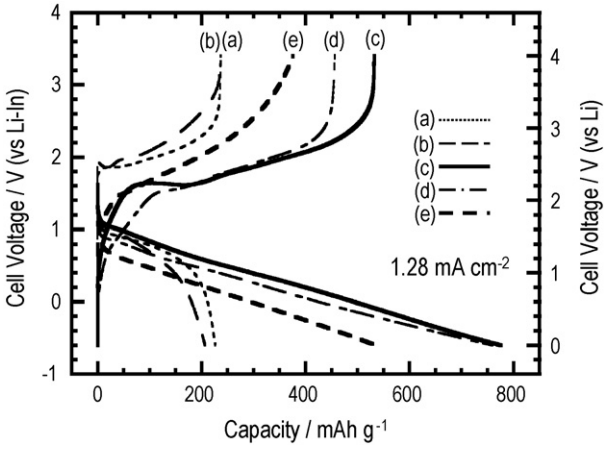

Fig. 3. The charge–discharge curves at 1.28 mA cm^{-2} of the cells with the nanocomposite electrode and the hand-mixed-electrode; the amount of the acetylene black in the nanocomposite (a), (b), (c) and (d) are 0, 4, 6 and 8 wt.%, respectively. The hand-mixed-electrode (e) contains 6 wt.% acetylene black.

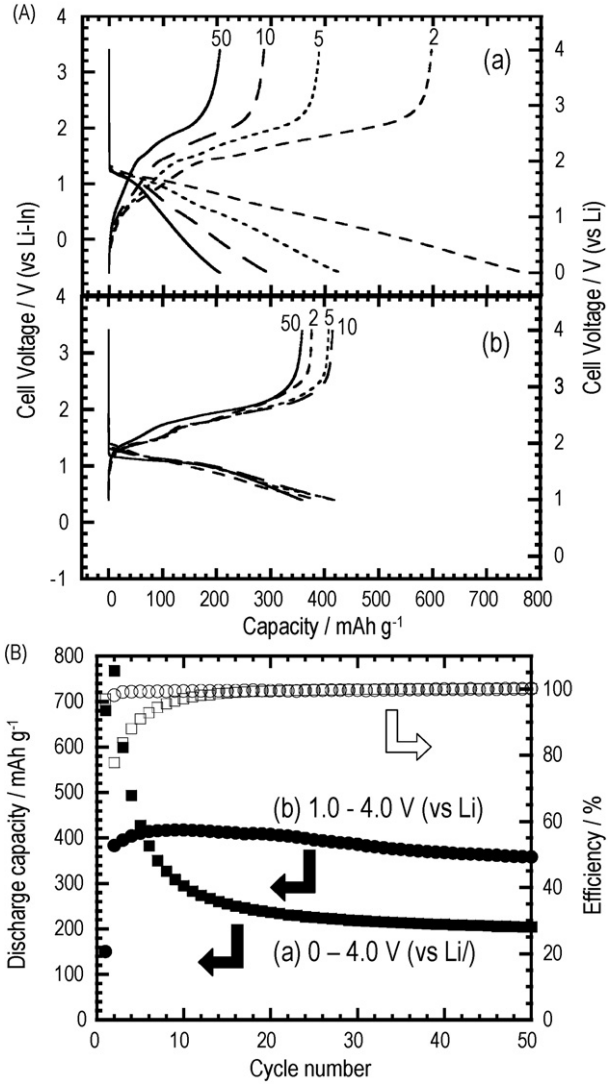

Fig. 4. The charge–discharge curves (A) and the cycle performance (B) at 1.28 mA cm^{-2} of the cells with the nanocomposite containing 6 wt.% acetylene black in the voltage range (a) 0–4.0 V and (b) 1.0–4.0 V vs. Li.

cell capacities are about 200 mAh g^{-1}. The capacity of the cell using the nanocomposite with 6 wt.% AB is much higher than that with 0 and 4 wt.% AB. Although the discharge capacity of the nanocomposite with 8 wt.% AB is almost the same as that with 6 wt.% AB, the charge capacity of the cell using the nanocomposite with 8 wt.% AB is lower than that with 6 wt.% AB. The addition of 6 wt.% AB to the nanocomposite is appropriate to form electron and lithium-ion conduction paths. The discharge voltage and capacity of the cell using the nanocomoposite electrode (c) is higher than those of the cell with the hand-mixed-electrode (e). This suggests that the formation of a favorable interface and the increase of contact area improve the electrochemical performance of the cell using the nanocomposite electrode.

The cycle performances of the cells with the NiS–80Li_2S·20P_2S_5-AB (6 wt.%) nanocomposite electrode at 1.28 mA cm^{-2} are shown in Fig. 4. Two cutoff voltages were used: (a) 0–4.0 V vs. Li and (b) 1.0–4.0 V vs. Li. The initial discharge capacity of the cell with the nanocomposite electrode at the cutoff voltage of 0 V is 775 mAh g^{-1}, which is larger than the theoretical capacity of NiS. The discharge capacity of the cell decreases rapidly during initial 10 cycles and then the cell retains 200 mAh g^{-1} for consecutive 40 cycles at the

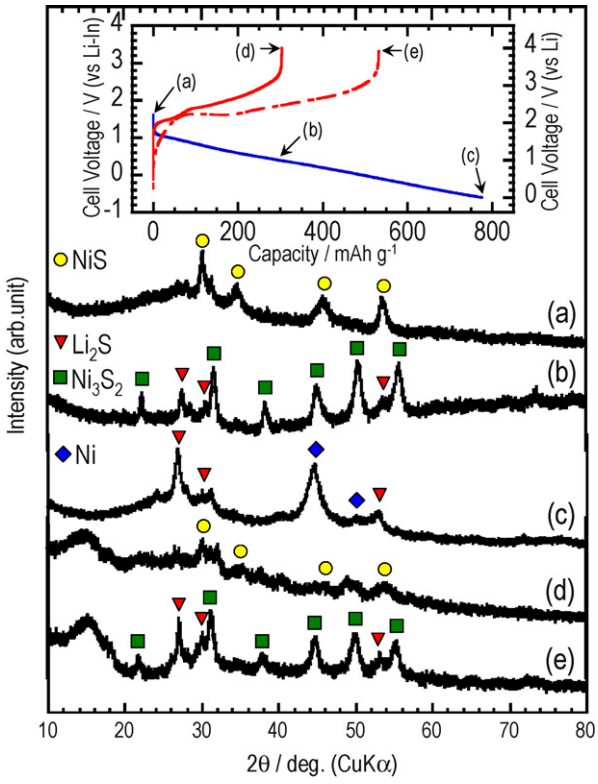

Fig. 5. The ex situ XRD patterns of the nanocomposite electrode after discharged and charged: (a) before discharge, (b) after discharge to 1.0 V, (c) after discharge to 0 V, (d) after charge from 1.0 to 4.0 V and (e) after charge from 0 to 4.0 V. The inset is the charge–discharge curves in which the point of the *ex situ* XRD measurements are marked.

cutoff voltage 0–4.0 V. The cell with the nanocomposite at the cutoff voltage 1.0–4.0 V shows smaller capacity of 150 mAh g^{-1} at the first cycle but retains the reversible capacity of 360 mAh g^{-1} with the charge–discharge efficiency of almost 100% from the second cycle to the 50th cycle. The cycle performance of the cell with the nanocomposite is much better than that of the mixture because the cell with the hand-mixed-electrode at the cutoff voltage 1.0–4.0 V retained smaller capacity of 100 mAh g^{-1} for 50 cycles.

The *ex situ* XRD measurements of the NiS–80Li_2S·20P_2S_5-AB nanocomposite electrodes after charge and discharge were performed in order to investigate reaction mechanism of NiS in the nanocomposite. Fig. 5 shows the XRD patterns of the nanocomposite electrode before (a) and after discharge to 1.0 V (b) or 0 V (c); the patterns of the electrode after charge from 1.0 to 4.0 V (d) and from 0 to 4.0 V (e) are also shown in this figure. The XRD pattern before discharge (a) corresponds to the pattern of NiS. The XRD patterns due to Ni_3S_2 and Li_2S are observed after discharge to 1.0 V (b), while the patterns due to Ni and Li_2S are detected after discharge to 0 V (c). Broad XRD peaks appear after charge from 1.0 to 4.0 V (d); it is considered that the peaks are partially attributable to NiS and the pattern suggests the presence of other nickel sulfides. On the other hand, the XRD pattern after charge from 0 to 4.0 V (e) corresponds to the patterns of Ni_3S_2 and Li_2S. The initial discharge reaction mechanism of the all-solid-state cells using the nanocomposite electrode is similar to that of a Li/NiS cell with liquid and polymer electrolytes as mentioned above. From the viewpoints of reaction mechanism, we discuss the relationship between cutoff voltage and cell performance. It was reported that Ni nanoparticles were formed in the Li_2S matrix after discharge to 0 V in cells using a liquid electrolyte [4]. In the present case, the formation of Ni and Li_2S crystals were observed after discharge to 0 V. However, Ni_3S_2 and Li_2S crystals were formed instead of returning to the initial NiS crystal after charge to 4.0 V. The formation of a large amount of Li_2S matrix with quite low ionic and electronic conductivity is a possible reason for a large irreversible capacity and rapid capacity fading at the cutoff voltage 0–4.0 V. The reaction which causes a larger capacity than the theoretical capacity may be based on another reaction mechanism and, however, no trace of new crystalline compounds has not been detected by XRD measurements. It is concluded that the discharge–charge reaction between NiS and Ni_3S_2 shows a good cyclability in all-solid-state cells.

4. Conclusions

The NiS–80Li_2S·20P_2S_5 nanocomposite materials were prepared by a mechanical milling technique. NiS particles were much more dispersed in the NiS–80Li_2S·20P_2S_5 nanocomposite synthesized by mechanical milling than in the mixture of NiS and 80Li_2S·20P_2S_5 by mixing in mortar. The NiS particles in the nanocomposite were smaller than that in the mixture. These suggest that the contact area between the NiS active material and the 80Li_2S·20P_2S_5 electrolyte in the nanocomposite is larger than that in the mixture. The capacity of the cell with the nanocomposite electrode was larger than that with the hand-mixed-electrode at both current densities of 64 μA cm^{-2} and 1.28 mA cm^{-2}. The discharge voltage of the cell with the nanocomoposite electrode was higher than that with the hand-mixed-electrode, suggesting that the formation of the favorable interface improved the cell performance. The cycle performance at 1.28 mA cm^{-2} of the cell with the nanocomposite electrode was improved by changing cutoff voltage and was much better than that with the hand-mixed-electrode. The discharge capacity of the cell with the nanocomposite was 360 mAh g^{-1} after 50 cycles at 1.28 mA cm^{-2}. The reaction mechanism of the cell with the nanocomposite was basically in agreement with that of Li/NiS cells using a liquid electrolyte reported so far. The nanocomposite electrode reaction was not sufficiently reversible by discharging deeply. It is expected that the all-solid-state cell performance at higher current densities will be improved by use of an electrolyte matrix with higher Li^+ ion conductivity in the nanocomposite.

Acknowledgments

This work was supported by a Grant-in-Aid for Scientific Research from the Ministry of Education, Culture, Sports, Science and Technology of Japan, and also supported by the New Energy and Industrial Technology Development Organization (NEDO) of Japan.

References

[1] A. Hayashi, S. Hama, H. Morimoto, M. Tatsumisago, T. Minami, J. Am. Ceram. Soc. 84 (2001) 477.
[2] K. Takada, N. Aotani, K. Iwamoto, S. Kondo, Solid State Ionics 86 (1996) 877.
[3] F. Mizuno, A. Hayashi, K. Tadanaga, M. Tatsumisago, Solid State Ionics 177 (2006) 2731.
[4] A. Debart, L. Dupont, R. Patrice, J.-M. Tarascon, Solid State Sci. 8 (2006) 640.
[5] X. He, W. Pu, J. Ren, L. Wang, J. Wang, C. Jiang, C. Wan, Electrochim. Acta 52 (2007) 7372.
[6] X. Zhu, Z. Wen, Z. Gu, S. Huang, J. Electrochem. Soc. 153 (3) (2006) A504.
[7] S.-C. Han, H.-S. Kim, M.-S. Song, P.S. Lee, J.-Y. Lee, H.-J. Ahn, J. Alloys Compd. 349 (2003) 290.
[8] S.-C. Han, H.-S. Kim, M.-S. Song, J.-H. Kim, H.-J. Ahn, J.-Y. Lee, J. Alloys Compd. 351 (2003) 273.
[9] S.-C. Han, K.-W. Kim, H.-J. Ahn, J.-H. Ahn, J.-Y. Lee, J. Alloys Compd. 361 (2003) 247.
[10] A. Hayashi, Y. Nishio, H. Kitaura, M. Tatsumisago, Electrochem. Commun. 10 (2008) 1860.